This article was downloaded by: [Renmin University of China]
On: 13 October 2013, At: 10:21
Publisher: Taylor & Francis
Informa Ltd Registered in England and Wales Registered Number: 1072954 Registered office: Mortimer House, 37-41 Mortimer Street, London W1T 3JH, UK

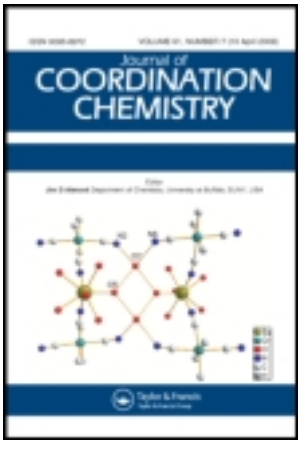

Journal of Coordination Chemistry
Publication details, including instructions for authors and subscription information:
http://www.tandfonline.com/loi/gcoo20

Cadmium(II) complexes of 4′-tolyl-2,2′:6′,2′′-terpyridine: synthesis, structures, and antibacterial activities

Lotf Ali Saghatforoush [a], Shane G. Telfer [b], Firoozeh Chalabian [c], Robabeh Mehdizadeh [a], Reza Golbedaghi [a] & Gholam Hossein Shahverdizadeh [d]

[a] Chemistry Department, Payame Noor University, 19395-4697, Tehran, Iran

[b] MacDiarmid Institute for Advanced Materials and Nanotechnology, Massey University, Palmerston North, New Zealand

[c] Department of Biology, Islamic Azad University, Tehran North Campus, Tehran, Iran

[d] Department of Chemistry, Azad Islamic University, Tabriz Branch, Tabriz, Iran

Published online: 01 Jul 2011.

To cite this article: Lotf Ali Saghatforoush, Shane G. Telfer, Firoozeh Chalabian, Robabeh Mehdizadeh, Reza Golbedaghi & Gholam Hossein Shahverdizadeh (2011) Cadmium(II) complexes of 4′-tolyl-2,2′:6′,2′′-terpyridine: synthesis, structures, and antibacterial activities, Journal of Coordination Chemistry, 64:12, 2186-2201, DOI: 10.1080/00958972.2011.591389

To link to this article: http://dx.doi.org/10.1080/00958972.2011.591389

PLEASE SCROLL DOWN FOR ARTICLE

Taylor & Francis makes every effort to ensure the accuracy of all the information (the "Content") contained in the publications on our platform. However, Taylor & Francis, our agents, and our licensors make no representations or warranties whatsoever as to the accuracy, completeness, or suitability for any purpose of the Content. Any opinions and views expressed in this publication are the opinions and views of the authors, and are not the views of or endorsed by Taylor & Francis. The accuracy of the Content should not be relied upon and should be independently verified with primary sources of information. Taylor and Francis shall not be liable for any losses, actions, claims, proceedings, demands, costs, expenses, damages, and other liabilities whatsoever or

howsoever caused arising directly or indirectly in connection with, in relation to or arising out of the use of the Content.

This article may be used for research, teaching, and private study purposes. Any substantial or systematic reproduction, redistribution, reselling, loan, sub-licensing, systematic supply, or distribution in any form to anyone is expressly forbidden. Terms & Conditions of access and use can be found at http://www.tandfonline.com/page/terms-and-conditions

Downloaded by [Renmin University of China] at 10:21 13 October 2013

Journal of Coordination Chemistry
Vol. 64, No. 12, 20 June 2011, 2186–2201

Taylor & Francis
Taylor & Francis Group

Cadmium(II) complexes of 4′-tolyl-2,2′:6′,2″-terpyridine: synthesis, structures, and antibacterial activities

LOTF ALI SAGHATFOROUSH*†, SHANE G. TELFER‡, FIROOZEH CHALABIAN§, ROBABEH MEHDIZADEH†, REZA GOLBEDAGHI† and GHOLAM HOSSEIN SHAHVERDIZADEH¶

†Chemistry Department, Payame Noor University, 19395-4697, Tehran, Iran
‡MacDiarmid Institute for Advanced Materials and Nanotechnology, Massey University, Palmerston North, New Zealand
§Department of Biology, Islamic Azad University, Tehran North Campus, Tehran, Iran
¶Department of Chemistry, Azad Islamic University, Tabriz Branch, Tabriz, Iran

(*Received 7 February 2011; in final form 5 May 2011*)

A straightforward synthetic method has been developed to prepare cadmium(II) complexes of 4′-tolyl-2,2′:6′,2″-terpyridine (ttpy) in good yields. These complexes are formulated as $\{[Cd(ttpy)(NO_3)_2][Cd_2(ttpy)_2(NO_3)_4]\}$ (**1**), $[Cd_2(ttpy)_2(N_3)_4]0.5CH_3OH \cdot 0.125H_2O$ (**2**), and $\{[Cd(ttpy)(SCN)(CH_3COO)][Cd(ttpy)(SCN)_2]_2\}$ (**3**). Intermolecular, intramolecular, hydrogen bonding and π–π stacking interactions were observed in the complexes, and are responsible for the arrangement of complexes in the crystal packing and play essential roles in forming different frameworks of **1**–**3**. The antibacterial activities of the synthesized complexes were tested against three gram positive bacteria and three gram negative bacteria.

Keywords: Terpyridine; Cadmium complexes; Antibacterial activity

Downloaded by [Renmin University of China] at 10:21 13 October 2013

1. Introduction

Terpyridine ligands have been known for nearly a century as effective complexing agents for a wide range of transition metal ions [1]. In the past few years, considerable attention has been drawn to the family of metal complexes having 2,2′:6′,2″-terpyridine (tpy) or substituted tpy components due to their structural advantage in drug design, materials chemistry, and as photofunctional supramolecular assemblies [2, 3]. The synthesis of tpy derivatives has been extensively studied by Constable's group, and a wide variety of substituted tpy compounds has been reported [4]. In the past few decades, special attention has been drawn to 4′-functionalized terpyridine ligands, since the appended substituents may be utilized not only to tailor the electronic properties of the ligand and its metal complexes, but also to incorporate new functionalities through further reactions [5, 6]. In 4′-tolyl-2,2′:6′,2″-terpyridine (ttpy), the 4′-tolyl substituent is electron donating and the extended conjugation makes ttpy a better π-acceptor ligand

*Corresponding author. Email: saghatforoush@gmail.com

ISSN 0095-8972 print/ISSN 1029-0389 online © 2011 Taylor & Francis
DOI: 10.1080/00958972.2011.591389

Downloaded by [Renmin University of China] at 10:21 13 October 2013

than terpyridine, such that it stabilizes the lower oxidation states. Also, the large surface area of the aromatic rings may generate π–π interactions in the solid state, potentially leading to high-dimensionality networks [6, 7]. Ttpy was first reported by Calzaferri and improved syntheses have since been described [8, 9]. Many of the reported metal complexes of ttpy have interesting redox and photophysical properties [10–13]. Despite the interest in ttpy as a ligand, its solid state structure was only reported in 2007 [14], and single-crystal structural details of only a few metal complexes have been documented [8, 15–17].

In previous work, we reported single-crystal structures of 4′-chloro-2,2′:6′,2″-terpyridine (tpyCl) with lead(II) salts including nine-, six-, five-, and four-coordinate Pb(II) complexes, $[Pb(tpyCl)(NO_3)_2]_n$, $[Pb(tpyCl)(ClO_4)_2]_n$, $[Pb(tpyCl)Br_2]_2$, and $[Pb(tpyCl)Cl][Pb(tpyCl)Cl_2][PbCl_3](CH_3OH)$ [18, 19]. This report is concerned with products formed by reacting cadmium(II) salts with ttpy in the presence of different anions. Cd(II) is known to have coordination numbers as high as eight [20]; thus in combination with ttpy we envisaged that some coordination sites of the metal may remain vacant. These complexes could serve as building blocks for the assembly of multi-functional coordination polymers or supramolecular networks exhibiting useful fluorescence and/or optoelectric properties [21, 22]. In this article we describe the synthesis and structural characterization of three Cd(II) complexes: $\{[Cd(ttpy)(NO_3)_2][Cd_2(ttpy)_2(NO_3)_4]\}$ (**1**), $[Cd_2(ttpy)_2(N_3)_4]0.5CH_3OH \cdot 0.125H_2O$ (**2**), and $\{[Cd(ttpy)(SCN)(CH_3COO)][Cd(ttpy)(SCN)_2]_2\}$ (**3**).

2. Experimental

2.1. *Materials and measurements*

4′-Tolyl-2,2′:6′,2″-terpyridine is commercially available from Aldrich and was used as received. All chemicals were of reagent grade and have been used without purification. FT-IR spectra (4000–400 cm^{-1}) were recorded with a Shimadzu FT-IR Prestige 21 spectrophotometer as KBr disks. Elemental analyses (C, H, and N) were performed using a Carlo ERBA model EA1108 analyzer. ^1H and ^{13}C NMR spectra were recorded on a 250 MHz Bruker spectrometer in d^6-DMSO. Electrospray mass spectra (ES-MS) were recorded in positive ion mode on a Waters Micromass ZMD mass spectrometer.

2.2. *X-ray crystallography*

X-ray diffraction data were collected on crystals with approximate dimensions of $0.20 \times 0.07 \times 0.07$ mm^3 for **1**, $0.20 \times 0.20 \times 0.20$ mm^3 for **2**, and $0.15 \times 0.10 \times 0.10$ mm^3 for **3**. Data were obtained at 123(2) K on a Rigaku Spider diffractometer, using a Rigaku VariMax-HF confocal optical system with monochromated Cu-Kα radiation ($\lambda = 1.54178$ Å). Crystal unit cell and orientation parameters were obtained from the auto-indexing procedure as implemented in the FS process. The structures have been solved by direct methods and refined by full-matrix least-squares on F^2 using SHELXL [23]. The molecular structure plots were prepared using ORTEP [24] and MERCURY [25]. Crystallographic data and details of the data collection and structure refinements are listed in table 1. Selected bond distances and angles are listed in table 2.

Downloaded by [Renmin University of China] at 10:21 13 October 2013

Table 1. Crystal data and structure refinements of **1**–**3**.

Identification code	**1**	**2**	**3**
Empirical formula	$C_{44}H_{34}Cd_2N_{10}O_{12}$	$C_{89}H_{72.50}Cd_4N_{36}O_{1.25}$	$C_{49}H_{37}Cd_2C_{10}N_9O_2S_3$
Formula weight	1119.61	2115.93	1104.86
Temperature (K)	123(2)	123(2)	123(2)
Wavelength (Å)	1.54178	1.54178	1.54178
Crystal system	Monoclinic	Monoclinic	Monoclinic
Space group	$P2_1/c$	$P2_1/n$	$P2_1/c$
Unit cell dimensions (Å, °)			
a	16.4170 (5)	21.5492(9)	20.3467(11)
b	19.9105 (5)	17.7040(6)	15.3652(7)
c	14.0078(6)	23.48250(1)	16.1380(9)
β	113.0130(2)	101.2120(2)	114.477(2)°
Volume (Å^3), Z	4214.4(4), 4	8788(3), 4	4591.8(4), 4
Calculated density (Mg m^{-3})	1.765	1.599	1.598
Absorption coefficient (mm^{-1})	8.766	8.223	9.104
$F(000)$	2240	4242	2216
Crystal size (mm^3)	0.20 × 0.07 × 0.07	0.20 × 0.20 × 0.20	0.15 × 0.10 × 0.10
θ range for data collection (°)	6.7–72.06	6.52–72.12	6.60–58.93
Limiting indices	$-19 \le h \le 19$; $-24 \le k \le 23$; $-12 \le l \le 15$	$-22 \le h \le 26$; $-21 \le k \le 16$; $-28 \le l \le 28$	$-22 \le h \le 21$; $-17 \le k \le 16$; $-16 \le l \le 17$
Reflections collected	48,192	74,903	44,445
Independent reflections	7887	16,664	6525
$I > 2\sigma(I)$	5528	13,018	4251
Absorption correction	Multi-scan	Multi-scan	Multi-scan
Max. and min. transmission	1.0 and 0.68	1.0 and 0.65	1.0 and 0.56
R_{int}	0.072	0.080	0.110
Refinement method	Full-matrix least-squares on F^2	Full-matrix least-squares on F^2	Full-matrix least-squares on F^2
Data/restraints/parameters	7887/144/634	16,664/102/1169	6525/0/589
Goodness-of-fit on F^2	1.113	1.113	0.999
Final R indices [$I > 2\sigma(I)$]	$R_1 = 0.0540$; $wR_2 = 0.1219$	$R_1 = 0.0578$; $wR_2 = 0.1602$	$R_1 = 0.0532$; $wR_2 = 0.1112$
R indices (all data)	$R_1 = 0.0729$; $wR_2 = 0.1318$	$R_1 = 0.0686$; $wR_2 = 0.1726$	$R_1 = 0.0765$; $wR_2 = 0.1266$
Largest difference Peak and hole (e Å^{-3})	1.476 and −1.878	0.962 and −0.994	0.990 and −1.142

Table 2. Selected bond lengths (Å) and angles (°) for **1**–**3**.

1		**2**		**3**	
Cd1–O2	2.285(4)	Cd1–N120	2.215(7)	Cd1–N100	2.224(7)
Cd1–N2	2.296(4)	Cd1–N60	2.343(5)	Cd1–N3	2.313(5)
Cd1–O5	2.323(4)	Cd1–N1	2.357(5)	Cd1–N2	2.330(5)
Cd1–N1	2.361(4)	Cd1–N2	2.358(5)	Cd1–N1	2.337(5)
Cd1–N3	2.372(4)	Cd1–N50	2.382(6)	Cd1–O3	2.346(4)
Cd1–O4	2.568(4)	Cd1–N3	2.429(5)	Cd1–O2	2.371(4)
Cd2–N22	2.317(4)	Cd2–N40	2.251(6)	Cd2–N5	2.296(5)
Cd2–O21	2.337(4)	Cd2–N50	2.276(5)	Cd2–N99	2.328(7)
Cd2–N23	2.377(4)	Cd2–N5	2.323(4)	Cd2–N4	2.342(5)
Cd2–N21	2.391(4)	Cd2–N4	2.365(5)	Cd2–N6	2.362(5)
Cd2–O25	2.446(4)	Cd2–N6	2.374(5)	Cd2–N88	2.365(6)
Cd2–O24A	2.476(5)	Cd2–N60	2.396(5)	Cd2–S88	2.6303(2)
O2–Cd1–O5	85.47(15)	N120–Cd1–N60	86.9(2)	N100–Cd1–N3	101.6(2)
O2–Cd1–N1	96.71(16)	N60–Cd1–N1	90.91(18)	N100–Cd1–N2	109.4(2)
N2–Cd1–N1	70.50(14)	N1–Cd1–N50	90.05(19)	N100–Cd1–N1	91.70(19)
N2–Cd1–N3	69.25(14)	N2–Cd1–N50	87.92(16)	N3–Cd1–O3	116.53(16)
O5–Cd1–N3	83.46(13)	N120–Cd1–N3	90.5(2)	N2–Cd1–O3	115.46(15)
N1–Cd1–O4	77.97(13)	N2–Cd1–N3	67.90(16)	N1–Cd1–O3	82.85(15)
N3–Cd1–O4	134.97(14)	N120–Cd1–N2	115.4(3)	N3–Cd1–O2	89.47(16)
N22–Cd2–N23	69.90(15)	N120–Cd1–N50	152.4(3)	N5–Cd2–N99	92.01(18)
O21–Cd2–N23	92.27(14)	N40–Cd2–N50	91.9(2)	N99–Cd2–N4	99.66(19)
N22–Cd2–N21	69.10(14)	N40–Cd2–N4	96.24(19)	N99–Cd2–N6	87.11(19)
N21–Cd2–O25	80.91(14)	N40–Cd2–N6	91.36(18)	N5–Cd2–N88	96.97(18)
N23–Cd2–O24A	76.65(16)	N50–Cd2–N6	98.47(18)	N4–Cd2–N88	88.21(19)
N21–Cd2–O24A	125.58(16)	N40–Cd2–N60	167.67(18)	N6–Cd2–N88	91.40(19)
O25–Cd2–O24A	73.20(16)	N50–Cd2–N60	76.00(18)	N99–Cd2–S88	81.59(14)
O21–Cd2–O25	87.21(13)	N5–Cd2–N60	88.57(16)	N88–Cd2–S88	89.74(13)

ISOR restraints were applied to all nitrogens and oxygens in structure **1** to produce chemically reasonable thermal ellipsoids. SIMU restraints for all nitrogens, a bond angle restraint for one of the azides, and bond distance restraints for MeOH were applied in structure **2**.

2.3. *Synthesis*

2.3.1. Preparation of {[Cd(ttpy)(NO$_3$)$_2$][Cd$_2$(ttpy)$_2$(NO$_3$)$_4$]} (1). 4′-Tolyl-2,2′:6′,2″-terpyridine (0.323 g, 1.0 mmol) was placed in one arm of a branched tube and cadmium(II) nitrate (0.308 g, 1.0 mmol) in the other. Methanol was carefully added to fill both arms, the tube was then sealed and the ligand-containing arm was immersed in a bath at 60°C while the other remained at ambient temperature. After 6 days, the crystals had deposited in the cooler arm were filtered off, washed with diethylether, and air-dried. Yield: 82.5%. Analysis: Found (%): C: 47.39, H: 2.86, N: 12.71. Calcd $C_{44}H_{34}Cd_2N_{10}O_{12}$ (%): C: 47.16, H: 3.04, N: 12.50. IR (cm^{-1}): 3047(w), 2950(w), 1581(s), 1573(m), 1558(s), 1530(m), 1476(s), 1390(vs), 815(m), 670(m). ES-MS: m/z 1057 $[Cd_2(ttpy)_2(NO_3)_3]^+$, 497 $[Cd(ttpy)(NO_3)]^+$. ^{1}H-NMR (DMSO): δ 9.051 (d, 2H), 8.92 (s, 2H), 8.61 (br s, 2H), 8.360 (t, 2H), 8.08 (d, 2H), 7.832 (m, 2H), 7.485 (d, 2H), 3.337 (s, 3H) ppm. ^{13}C NMR (DMSO): δ 155.37, 152.83, 149.87 (2C), 143.58, 135.18, 131.08, 129.14, 126.93 (2C), 124.19, 120.90, 22.96 ppm.

Downloaded by [Renmin University of China] at 10:21 13 October 2013

Downloaded by [Renmin University of China] at 10:21 13 October 2013

2.3.2. Preparation of $[Cd_2(ttpy)_2(N_3)_4]0.5CH_3OH \cdot 0.125H_2O$ (2). 4′-Tolyl-2,2′:6′,2″-terpyridine (0.323 g, 1.0 mmol) was placed in one arm of a branched tube and cadmium(II) acetate (0.264 g, 1.0 mmol) and sodium azide (0.13 g, 2.0 mmol) in the other. Methanol was carefully added to fill both arms. After 4 days, the crystals deposited in the cooler arm were filtered off, washed with diethylether, and air-dried. Yield: 88%. Analysis: Found (%): C: 50.71, H: 3.24, N: 24.10. Calcd for $C_{89}H_{72.50}Cd_4N_{36}O_{1.25}$ (%): C: 50.47, H: 3.43, N, 23.82. IR (cm^{-1}): 3050(w), 2930(w), 2050(m), 1581(s), 1573(m), 1558(s), 1476(s), 820(m). ES-MS: m/z 1016 $[Cd_2(ttpy)_2(N_3)_3]^+$. ^1H NMR (DMSO): δ 9.084 (m, 4H), 8.833 (d, 2H), 8.762 (t, 2H), 8.256 (t, 2H), 8.102 (d, 2H), 7.422 (d, 2H), 3.16 (s, 3H) ppm. ^{13}C NMR (DMSO): δ 155.91, 154.52, 150.38, 141.26, 139.87, 135.18, 129.42, 129.16, 127.33, 124.24, 121.81, 120.67, 22.17 ppm.

2.3.3. Preparation of $\{[Cd(ttpy)(SCN)(CH_3COO)][Cd(ttpy)(SCN)_2]_2\}$ (3). Complex **3** was synthesized in the same way as **2** using potassium thiocyanate instead of sodium azide. Yield: 80.5%. Analysis: Found (%): C: 52.96, H: 3.45, N: 11.61. Calcd for $C_{49}H_{37}Cd_2N_9O_2S_3$ (%): C: 53.22, H: 3.35, N: 11.40. IR (cm^{-1}) selected bonds: 3018(w), 2870(w), 2113(m), 2076(w), 1580(s), 1558(s), 1476(s), 852(m). ES-MS: m/z 1046 $[Cd_2(ttpy)_2(SCN)_3]^+$, 494 $[Cd(ttpy)(CH_3COO)]^+$, 493 $[Cd(ttpy)(SCN)]^+$. ^1H NMR (DMSO): δ 8.927 (m, 4H), 8.748 (d, 2H), 8.305 (t, 2H), 8.174 (d, 2H), 7.875 (m, 2H), 7.566 (d, 2H), 3.418 (s, 3H), 2.48 (s, 3H). ^{13}C NMR (DMSO): δ 179.77, 153.88 (2C), 153.54, 142.08, 141.34, 140.05, 135.44, 132.61, 129.05, 125.68, 123.84, 121.43, 40.96, 22.41 ppm.

2.4. *Antibacterial activity test*

In vitro activity test was carried out using the growth inhibitory zone (well method) [26, 27]. The potency of components was determined against three Gram-positive bacteria: *Streptococcus pyogenes* (RITCC 1940), *Staphylococcus aureus* (RITCC 1885), and *Bacillus anthracis* (RITCC 1036), and also against the three Gram-negative bacteria: *Klebsiella pneumonia* (RITCC 1249), *Escherichia coli* (RITCC 1330), and *Pseudomonas aeruginosa* (RITCC 1547). Microorganisms (obtained from enrichment culture of the microorganisms in 1 mL Muller–Hinton broth incubated at 37°C for 12 h) were cultured on Muller–Hinton agar medium. The inhibitory activity was compared with that of standard antibiotics, such as gentamicin (10 μg). After drilling wells on the medium using a 6 mm cork borer, 100 μL of solution from different compounds was poured into each well. The plates were incubated at 37°C overnight. The diameter of the inhibition zone was measured as precisely as possible. Each test was carried out in triplicate and the average was calculated for inhibition zone diameters. A blank containing only methanol showed no inhibition in a preliminary test. The macrodilution broth susceptibility assay was used for the evaluation of minimal inhibitory concentration (MIC). The use of 12 test tubes is required by the macro-dilution method. By including 1 mL Muller–Hinton broth in each test, and then adding 1 mL extract with concentration 100 mg mL^{-1} in the first tube, we made a serial dilution of this extract from the first tube to the last tube. Bacterial suspensions were prepared to match the turbidity of 0.5 McFarland turbidity standards. Matching this turbidity provided bacterial inoculums concentration of 1.5×10^8 cfu mL^{-1}. Then 1 mL of bacterial

suspension was added to each test tube. After incubation at 37°C for 24 h, the last tube was determined as the MIC without turbidity.

3. Results and discussion

3.1. *Spectroscopy*

IR spectra for **1**–**3** contain characteristic C=N and C=C vibrational frequencies for free ligand at 1400–1600 cm^{-1}. The strong ν_{as}(SCN) absorption at 2137 cm^{-1} for **3** shows the presence of 1,3-μ-thiocyanate and the peak at 2076 cm^{-1} is indicative of terminal nitrogen coordination [28, 29]. In **2**, $\nu_{as}(N_3)$ appears as a very strong split band at 2050 and 2037 cm^{-1}, assigned to both end-on bridging and terminal azide [29, 30]. The presence of coordinated nitrate as chelating bidentate and bridging ligand on **1** is associated with absorptions at 1390 and 1530 cm^{-1} [19, 29]. The ^{1}H NMR spectra of **1**–**3** dissolved in DMSO display seven resonances in the downfield region of the spectrum that can be assigned to protons of ttpy. One singlet at 3.160–3.418 ppm is assigned to methyl of the ttpy ligand. In **3**, a further singlet at 2.48 ppm is assigned to methyl of acetate. The ^{13}C NMR spectra of **1**–**3** in DMSO display resonances assigned to the aromatic carbons of pyridine of ttpy. The aliphatic carbon of the methyls is at 22.17–22.96 ppm [31].

3.2. *Crystal structure of {[Cd(ttpy)(NO$_3$)$_2$][Cd$_2$(ttpy)$_2$(NO$_3$)$_4$]} (1)*

The reaction of ttpy with $Cd(NO_3)_2$ in methanol gave pale orange crystals of **1** that were suitable for X-ray diffraction analysis. Crystals of **1** belong to the space group $P2_1/c$. The crystallographic data and refinement parameters are summarized in table 1 and selected bond parameters are listed in table 2. An ORTEP plot of the molecular structure of **1** is presented in figure 1. The structure determination revealed that two

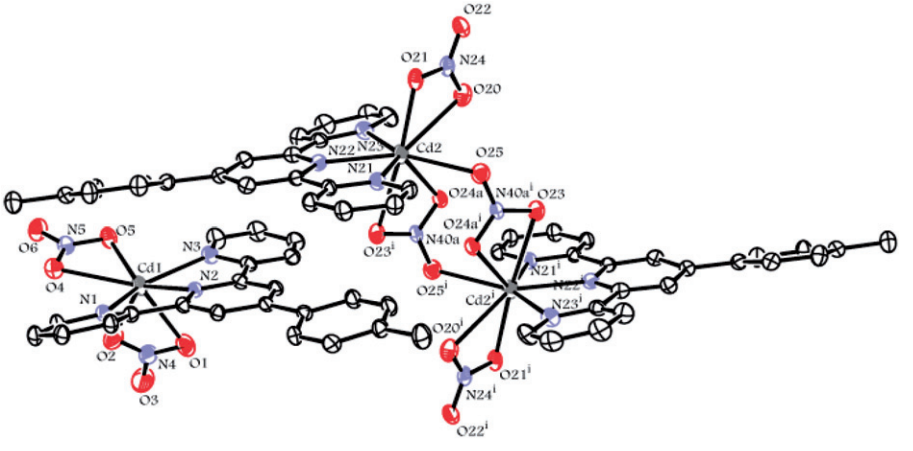

Figure 1. ORTEP plot for **1** with 50% thermal ellipsoids (hydrogens are omitted for clarity); i: $-x, y+1/2, -z+1/2$.

Downloaded by [Renmin University of China] at 10:21 13 October 2013

Downloaded by [Renmin University of China] at 10:21 13 October 2013

separate coordination entities were present in the asymmetric unit. One of these is a seven-coordinate mononuclear species [Cd(ttpy)$(NO_3)_2$], in which three nitrogens of ttpy and four oxygens of two nitrates were coordinated to Cd(II). The other is an eight-coordinate dinuclear species [(ttpy)(NO_3)Cd(μ-$NO_3)_2$Cd(ttpy)(NO_3)], the two halves of which are related by an inversion center. Here, the three nitrogens of ttpy and five oxygens of three nitrates coordinate to Cd(II) with N_3O_5 coordination spheres. As can be seen from figure 1, nitrates coordinate in both terminal bidentate (η^2) and bridging ($\eta^2:\eta^1$) modes. The bridging nitrate is disordered over two positions with an occupancy ratio of 3 : 1. Each ttpy is tridentate chelating in both the mononuclear and dinuclear complexes, forming five-membered Cd–N–C–C–N metallacycles with mean N1–Cd1–N2, N2–Cd1–N3, and N21–Cd2–N22, N22–Cd2–N23 angles of 70.50°, 69.25°, 69.11°, and 69.87°, respectively. The central pyridine ring of the mononuclear species (C6, C7, C8, C9, C10, N2) forms a dihedral angle of 6.36° with the metallacycle plane (Cd1, N1, C5, C6, N2) and an angle of 5.91° with the other plane (Cd1, N2, C10, C11, N3), showing that the three connected planes are far from coplanarity. However, the central pyridine of the dinuclear species (C35, C36, C37, C38, C39, N22) forms a dihedral angle of 2.02° with the metallacycle plane (Cd2, N21, C34, C35, N22) and an angle of 1.34° with the other plane (Cd1, N22, C39, C40, N23), showing that the three connected planes are not far from coplanarity. Some of the N–O bond distances are unusually long (2.761(5); 2.568(3) and 2.729(4); 2.675(4) Å in the mononuclear and dinuclear complexes, respectively) [20]. The Cd–N bond distances are very similar to related complexes with the bond to the central pyridyl ring being shorter than those to terminal rings [7a, 20, 32]. This pattern has been attributed to the constrained bite of terpyridyl [33]. The methyl phenyl substituent is not coplanar with the central pyridine ring of the tpy motif, but is twisted such that it makes a dihedral angle of 8.98° and 16.48° for mononuclear and dinuclear complexes, respectively. The tpy metal-binding domain is approximately planar with interplanar angles between bonded pyridine rings of less than 9.9° for dimer and 12.50° for monomer. The Cd···Cd distance within the dimer is 5.272 Å. The bond lengths of the three N–O bonds and also the three bond angles for nitrate in the mononuclear and dinuclear species are different, showing that the nitrates have been distorted in forming a bridge between two cadmiums.

Intermolecular and intramolecular hydrogen bonding and π–π interactions are observed in **1**. An inspection of **1** for weak directional intermolecular interactions by the program MECURY, used for showing supramolecular interactions, shows that there are O···H–C interactions [19, 34, 35] (table 3 and figure 2). The C–H···$O^{nitrate}$ separations range from 2.412 to 2.606 Å, which is indicative of moderate to strong hydrogen bonds [19, 36]. Such a combination of noncovalent bonds could be exploited to design anion receptors [19, 37]. All the terpyridine molecules are parallel in the crystal packing of **1**, forming a layered packing structure with interlayer distances of 3.648 Å and 4.646 Å [19, 38]. The centroid to centroid separations between neighboring pyridine rings (3.351–3.386 Å) are indicative of offset π–π interactions. The π–π interactions in this structure are highlighted in figure 2.

3.3. *Crystal structure of [Cd_2(ttpy)$_2$(N_3)$_4$]0.5CH_3OH·0.125H_2O (2)*

[Cd_2(ttpy)$_2$(N_3)$_4$] crystallizes in the monoclinic space group $P2_1/n$. Crystal data and details of the structure determination for **2** are given in table 1, an ORTEP plot of the

Table 3. Intermolecular interactions in crystals of **1**–**3**.

A···H–B	H···A (Å)	B···A (Å)	B–H···A (°)
1			
O20···H50–C50($-x$, y, $-z+1/2$)	2.606	3.531(2)	164.63
O21···H7–C7($x+1/2$, $-y+1/2$, $z+1/2$)	2.593	3.427(2)	146.63
O21···H21–C21($x+1/2$, $y+1/2$, z)	2.412	3.326(1)	161.48
O23···H9–C9($-x+1/2$, $y+1/2$, $-z+1/2$)	2.469	3.356(1)	155.25
O23···H12–C12($-x$, $-y$, $-z$)	2.513	3.346	146.48
O23···H17–C17($-x$, $-y$, $-z$)	2.453	3.387	167.66
O1···H38–C38($-x$, $-y$, $-z$)	2.495	3.417	136.35
O1···H4–C41($-x$, $-y$, $-z$)	2.526	3.339	143.50
O2···H43–C43($-x$, $-y$, $-z$)	2.488	3.188	130.54
O6···H51A–C51($-x$, $-y$, $-z$)	2.520	3.490	170.65
N40B···H17–C17($-x$, y, $-z+1/2$)	2.575	3.458(2)	154.72
N24···H50–C50($-x$, y, $-z+1/2$)	2.593	3.370(2)	139.37
N4···H41–C41($-x$, y, $-z+1/2$)	2.598	3.340(2)	135.23
$\pi\cdots\pi$ (Slipped face-to-face) C34···C21	–	3.351	–
C34···C17		3.386	
2			
N40···H9–C9($x+1/2$, $-y+1/2$, $z+1/2$)	2.541	3.434(8)	156.70
N40···H12–C12($x+1/2$, $-y+1/2$, $z+1/2$)	2.502	3.430(8)	165.57
N40···H17–C17($x+1/2$, $-y+1/2$, $z+1/2$)	2.620	3.469(8)	149.03
N41···H17–C17($x+1/2$, $-y+1/2$, $z+1/2$)	2.601	3.442(8)	147.71
N41···H82A–C82($x+1/2$, $-y+1/2$, $z+1/2$)	2.582	3.073(8)	91.49
N42···H63–C63($x+1/2$, $-y+1/2$, $z+1/2$)	2.550	3.121(8)	118.81
N42···H35–C35($x+1/2$, $-y+1/2$, $z+1/2$)	2.320	3.211(8)	156.03
N52···H91–C91($x+1/2$, $-y+1/2$, $z+1/2$)	2.627	3.447(8)	144.78
N92···H51–C51($x+1/2$, $-y+1/2$, $z+1/2$)	2.433	3.354(8)	163.48
N92···H48–C48($x+1/2$, $-y+1/2$, $z+1/2$)	2.645	3.569(8)	164.66
N92···H81–C81($x+1/2$, $-y+1/2$, $z+1/2$)	2.579	3.502(8)	164.18
N91···H81–C81($x+1/2$, $-y+1/2$, $z+1/2$)	2.587	3.360(8)	138.78
N90···H72–C72($x+1/2$, $-y+1/2$, $z+1/2$)	2.624	3.515(8)	156.69
N90···C200S($x+1/2$, $-y+1/2$, $z+1/2$)		2.848	
N72···H71–C71($x+1/2$, $-y+1/2$, $z+1/2$)	2.598	3.506(8)	159.96
N120···H61–C61($x+1/2$, $-y+1/2$, $z+1/2$)	2.552	3.490(8)	169.64
$\pi\cdots\pi$ (Slipped face-to-face) C52···C74	–	3.247	–
$\pi\cdots\pi$ (Slipped face-to-face) C55···C91	–	3.278	–
$\pi\cdots\pi$ Centroid C16–C21···C23–C27N4		3.924	
3			
O3···H49–C49($-x$, y, $-z+1/2$)	2.609	3.229(2)	123.17
O3···H48–C48($-x$, y, $-z+1/2$)	2.359	3.221(2)	150.60
O3···H40–C40($-x$, y, $-z+1/2$)	2.577	3.473(2)	157.02
O2···H14–C14($-x$, y, $-z+1/2$)	2.250	3.185(2)	167.32
N99···H41–C41($-x$, y, $-z+1/2$)	2.538	3.319(2)	139.65
S100···H45–C45	2.919		
S100···H33–C33	2.916		
C100···H45–C45	2.719		
C88···H4–C4	2.640	3.543	158.90
$\pi\cdots\pi$ (Slipped face-to-face) C70···C49	–	3.377	–
$\pi\cdots\pi$ (Slipped face-to-face) C8···C50	–	3.360	–
Centroid C44–C50···C11–C15N3		3.745	
Centroid C35–C48N5···C6–C10N2		3.643	

molecular structure of **2** is depicted in figure 3, and some selected interatomic bond distances and angles listed in tables 2 and 3.

The asymmetric unit of **2** comprises two independent dinuclear $[Cd_2(ttpy)_2(N_3)_4]$ complexes along with methanol (disordered over two positions) and water.

Downloaded by [Renmin University of China] at 10:21 13 October 2013

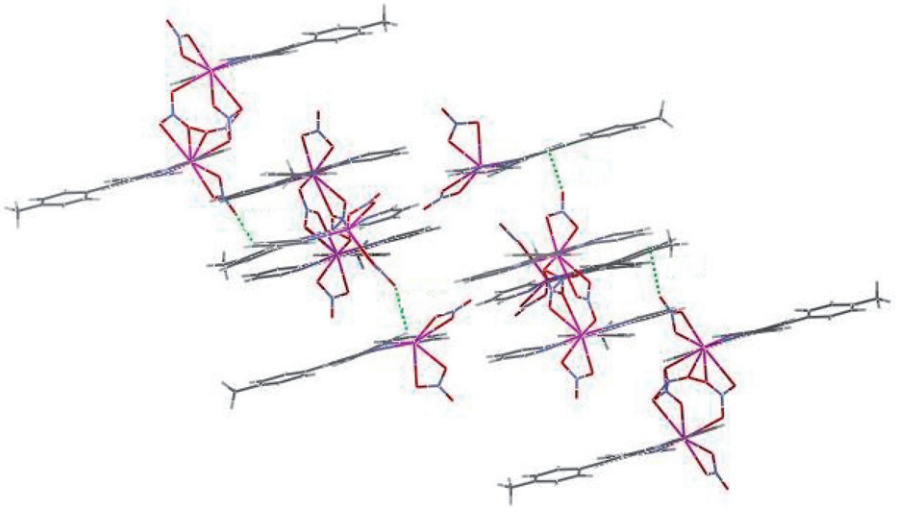

Figure 2. View of the stacking layers in **1** along the *b*-direction.

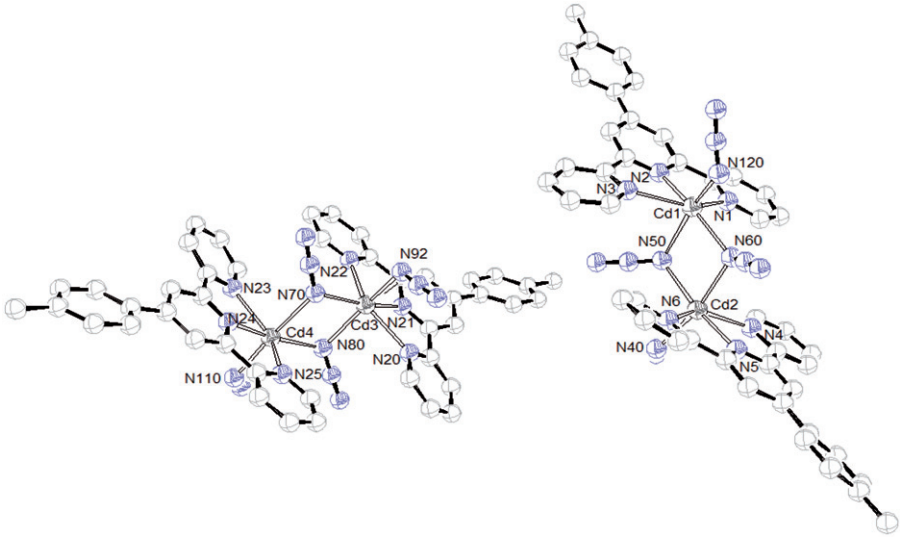

Figure 3. ORTEP plot for **2** with 30% thermal ellipsoids (hydrogens are omitted for clarity).

Each centrosymmetric dimer consists of Cd(II) ions coordinated to tridentate ttpy lignds and linked by two end-on bridging azides. The remaining two azides are terminal ligands. Each cadmium is located in a distorted octahedral coordination environment. The Cd1 ··· Cd2 and Cd3 ··· Cd4 distances are 3.713 and 3.720 Å, respectively. The Cd–N distances to the bridging azide range from 2.276 to 2.395 Å, and the distances to terminal azides are Cd(1)–N(120), 2.215; Cd(2)–N(40), 2.252; Cd3–N(92), 2.271; and Cd(4)–N(110), 2.290 Å. The Cd–N distances to ttpy vary between 2.323 and 2.428 Å. The Cd–N bond distances mostly match those observed in analogous CdN6

Downloaded by [Renmin University of China] at 10:21 13 October 2013

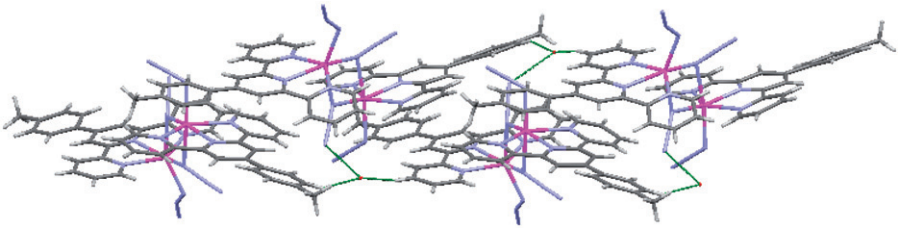

Figure 4. View of the stacking layers in **2** along the *c*-direction, showing the hydrogen bonding.

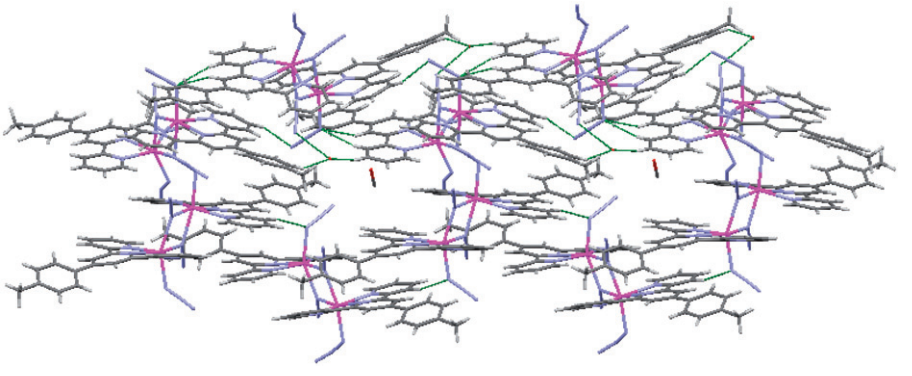

Figure 5. View of the stacking layers in **2** along the *a*-direction.

Downloaded by [Renmin University of China] at 10:21 13 October 2013

complexes [39–43]. The bridging angles are very similar, [Cd(1)–N(60)–Cd(2), 103.20; Cd(1)–N(50)–Cd(2), 105.71; Cd(3)–N(70)–Cd(4), 105.25; and Cd(3)–N(80)–Cd(4), 106.82°]. The bridging azides are very close to linear with an average N_α–N_β–N_γ angle of 177.65°; however, the terminal azides have an average N_α–N_β–N_γ angle of 166.31°. The N_α–N_β bond lengths [1.073(9)–1.195(7) Å] are a little shorter than those of N_β–N_γ [1.182(8)–1.209(12) Å], where N_α indicates the nitrogen coordinated to cadmium(II). These variations in bond distances have also been observed for azides bonded in a terminal or μ_2-1,1-bridging fashion [5, 39–42].

One water and methanol are not coordinated to cadmium. The hydrogen of uncoordinated water is involved in hydrogen bonding. The dimers by hydrogen bonding of water form a 1D network (figure 4). There are intermolecular π–π [43, 44] interactions between aromatic rings of the ttpy ligands with a centroid–centroid distance of 3.589 Å. There are some weak C–H···aromatic interactions, C4–H4···Cg1, C43–H43···Cg2, and C53-H53···Cg3 with interaction distances of 2.849 Å, 2.922 Å, and 3.047 Å, where the Cg1 is the ring of C90–96, Cg2 is the ring of C74–80 and the Cg3 is the ring of C1–C5/N3. The C–H aromatic interactions and π–π stacking interactions play important roles in the packing of the dimers (figure 5).

3.4. *Crystal structure of {[Cd(ttpy)(SCN)(CH$_3$COO)][Cd(ttpy)(SCN)$_2$]$_2$} (3)*

The reaction of ttpy with $Cd(CH_3COO)_2 \cdot 4H_2O$ and KSCN in methanol gave brown crystals that were suitable for X-ray diffraction analysis. Crystal data and details of the

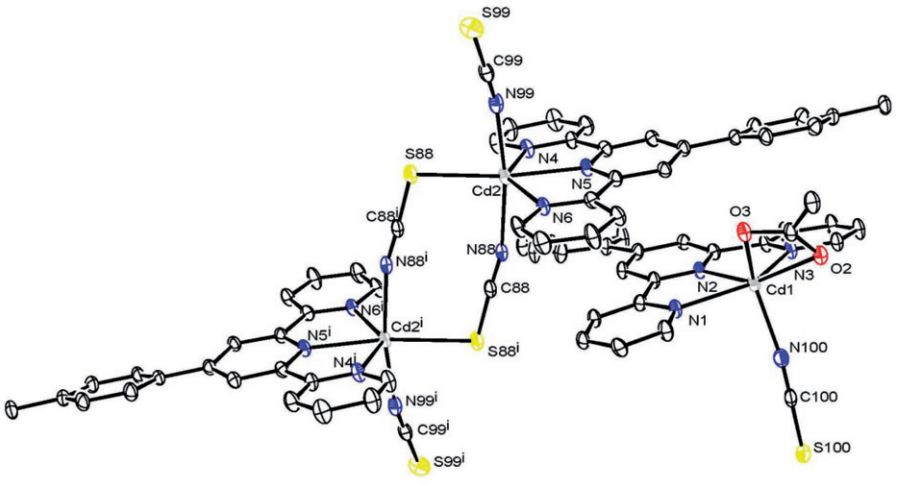

Figure 6. ORTEP plot for **3** with 30% thermal ellipsoids (hydrogens are omitted for clarity); i: $-x$, $y+1/2$, $-z+1/2$.

structure determination for **3** are given in table 1. Some selected interatomic bond distances and angles are listed in tables 2 and 3. An ORTEP plot of the molecular structure of **3** is depicted in figure 6.

Complex **3** crystallizes in the monoclinic space group $P2_1/c$. The structure determination unexpectedly reveals that two separate coordination entities were present in the unit cell. One of these was a six-coordinate mononuclear species, [Cd(ttpy)(SCN)(CH_3COO)], and the other was a six-coordinate dinuclear species, [(ttpy)(SCN)Cd(μ-SCN)$_2$Cd(ttpy)(SCN)].

In the mononuclear complex, Cd(II) centers are coordinated to a tridentate ttpy, nitrogen of SCN^- and two oxygens of a bidentate CH_3OO^- (figure 6). The Cd–N–C–C–N metallacycles involving ttpy have mean N1–Cd1–N2 and N2–Cd1–N3 angles of 68.58° and 68.97°, respectively. The central pyridine (C6, C7, C8, C9, C10, N2) forms a dihedral angle of 2.65° with the metallacycle plane (Cd1, N1, C5, C6, N2) and an angle of 3.12° with the other plane (Cd1, N2, C10, C11, N3). The tolyl substituent is not coplanar with the central pyridine ring of tpy, but is twisted with a dihedral angle of 14.50°. The tpy metal-binding domain is approximately planar with interplanar angles between bonded pyridine rings being less than 9.8°.

The structure of the centrosymmetric dinuclear complex is also shown in figure 6. In this case, Cd(II) adopts a distorted octahedral geometry with three nitrogens from ttpy, sulfur, and nitrogen from bridging SCN^-, and a nitrogen from a terminal SCN^- comprising the coordination sphere. The {Cd(μ-SCN-μ-NCS)Cd} core has Cd–S and Cd–N bond lengths of 2.630(2) and 2.366(7) Å, respectively. The Cd $\cdots$ Cd separation is 6.053 Å, which is somewhat longer than the intermetallic distances observed in similar species with azide or nitrate bridges. The other Cd–N and Cd–S distances fall in the range of 2.329–2.366 Å and 2.630 Å, respectively, which are normal [7a]. The SCN^- groups are nearly linear with N–C–S bond angles of 176.77–179.37°. The C–N–Cd and C–S–Cd linkages are bent and the related bond angles are in accord with similar reported complexes [7a, 16]. The Cd–N^{ttpy} bond lengths show the expected pattern for a

Downloaded by [Renmin University of China] at 10:21 13 October 2013

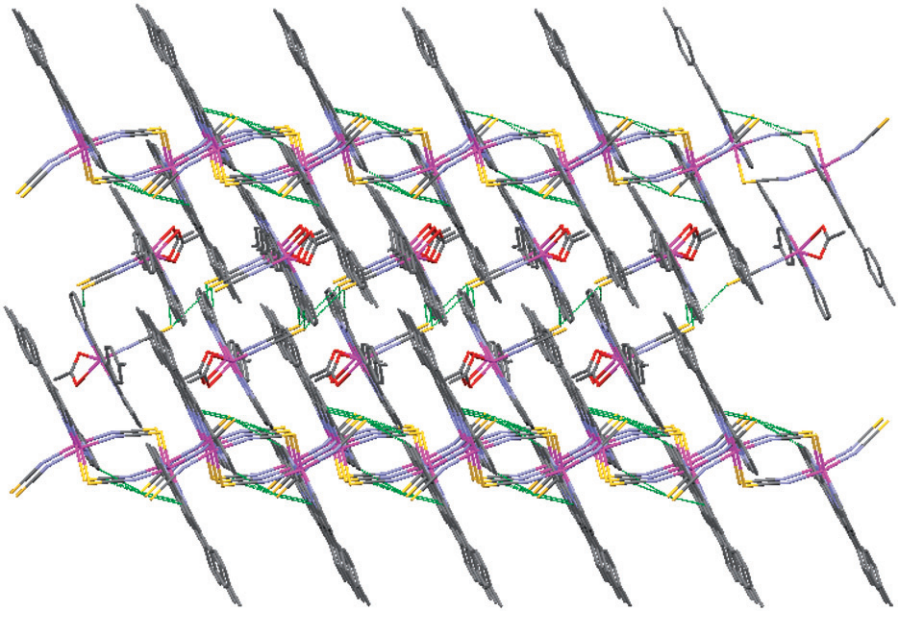

Figure 7. View of the stacking layers in **3** along the *b*-direction.

complex of 2,2′:6′,2″-terpyridine, with short contacts to central ring (2.297 Å) and longer contacts to the terminal rings (2.341–2.361 Å) [7, 18]. These bond lengths to the terminal rings very closely resemble those observed in other Cd–terpy complexes (2.337-2.360 Å), but the bond to nitrogen of the central pyridine ring of 2.297 Å is slightly shorter than those in the central ring of other Cd-terpy complexes (2.305–2.331 Å) [7]. This may be attributed to greater π-bonding with the 4-4′-methylphenyl substituted ligand. Once again, the methyl phenyl substituent is twisted with respect to the central pyridine ring of the terpy, with an angle of 14.77°. The terpy metal-binding domain is approximately planar with interplanar angles between bonded pyridine rings less than 6.40°.

An additional point of interest is the arrangement of the two complexes with respect to each other within the lattice, as presented in figure 7. There are clear intermolecular π–π interactions, with separation between two ligand planes of 3.59–3.70 Å. The following short contacts between N···H and O···H were observed in the complexes: N99–H41 (2.538 Å), O3–H40 (2.577 Å), O3–H48 (2.357 Å), O3–H49 (2.609 Å), and O2–H14 (2.250 Å). Specific short contacts between certain hydrogens of the terminal pyridine rings and sulfur and nitrogen of certain SCN^- ligands (S99···H31 (2.878 Å), S99···H42 (2.729 Å), S99···C42 (3.399 Å), S100···S100 (3.499 Å)) assist in building up a 3-D framework, as do contacts between oxygens of acetate and hydrogens of nearby complexes.

3.5. *A comparison of solid state and solution structures*

Although the X-ray crystal structure of **1** shows both a mononuclear and a dinuclear complex, only one ttpy-containing species is visible by NMR spectroscopy.

Downloaded by [Renmin University of China] at 10:21 13 October 2013

ES-MS verifies that a dinuclear species is present in solution, hence the NMR spectra can be explained by either a rapid equilibrium between the mononuclear and dinuclear complexes or dimerization of the mononuclear complex. The dinuclear structure of **2** is retained in solution, as evidenced by its ^{1}H and ^{13}C NMR spectra and its electrospray mass spectrum. With respect to **3**, again NMR spectroscopy indicates the presence of just one ttpy environment, which indicates that the mononuclear and dinuclear complex observed by X-ray crystallography are scrambled in solution. In this case, the simple dimerization of the mononuclear complex will not give the dinuclear complex since the latter complex does not contain acetate. Therefore, in this case it is most likely that a rapid exchange process renders the two complexes identical on the NMR timescale. This is consistent with the electrospray mass spectrometry results.

Downloaded by [Renmin University of China] at 10:21 13 October 2013

3.6. *Antibacterial activity*

The antibacterial activities of ttpy and **1**–**3** are shown in tables 4 and 5. The free ligand has appreciable activity against gram-positive bacteria *Escherichia coli* and *P. aeruginosa* (inhibitory zones ≥ 20 mm), but against *K. pneumonia* it shows reduced activity (inhibitory zones ≤ 15 mm) [45]. Among three tested gram-negative bacteria, the free ligand has good activity only against *B. anthracis*, while against *S. pyogenes* and *S. aureus* it is inactive. Complex **1** has weak activity against *B. anthracis* and *K. pneumonia*, while against other bacteria it is inactive. Complex **2** is active against all

Table 4. Antibacterial activities of ttpy and **1**–**3**.

Microorganism	Standard gentamicine	ttpy	Growth inhibitory zone (mm) Main compounds		
			1	**2**	**3**
S. Pyogenes(+)	13	–	–	20	–
B. Anthracis(+)	32	25	10	15	–
S. aureus(+)	20	–	–	20	–
E. coli(−)	25	25	–	20	–
K. pneumonia(−)	20	10	12	30	–
P. aeruginosa(−)	15	20	–	10	–

Table 5. Minimal inhibitory concentration (MIC).

Microorganism	ttpy	MIC (mg mL^{-1}) Main compounds		
		1	**2**	**3**
S. pyogenes(+)	–	–	50	–
B. anthracis(+)	12.5	100	100	–
S. aureus(+)	–	–	50	–
E. coli(−)	12.5	–	50	–
K. pneumonia(−)	100	100	6.25	–
P. aeruginosa(−)	50	–	100	–

tested gram-positive and gram-negative bacteria (inhibitory zones ≥ 20 mm), except *P. aeruginosa*, against which it shows slight activity. Complex **3** is inactive against all tested bacteria. As can be seen from tables 4 and 5, the antibacterial activity of **2** against *K. pneumonia* is higher than the free ligand. Though the free ligand is inactive against *S. pyogenes* and *S. aureus*, **2** shows good activity against these two kinds of gram negative bacteria. Also, the antibacterial activity of **2** against *K. pneumonia* and *S. pyogenes* is higher than the standard antibiotic gentamicine. The high antibacterial activity of **2** is probably due to N_3^- in this complex [46, 47]. The quantitative assays gave MIC values in the range of 6.25–100 mg mL^{-1} (table 5), which confirmed the above results.

Downloaded by [Renmin University of China] at 10:21 13 October 2013

4. Conclusions

Three new cadmium(II) complexes, $\{[Cd(ttpy)(NO_3)_2][Cd_2(ttpy)_2(NO_3)_4]\}$ (**1**), $[Cd_2(ttpy)_2(N_3)_4]0.5CH_3OH \cdot 0.125H_2O$ (**2**), and $[Cd(ttpy)(SCN)(CH_3COO)][Cd(ttpy)(SCN)_2]_2\}$ (**3**), were prepared and structurally characterized. The structures are interesting and different from each other. Coordination number of cadmium(II) in these complexes varies from eight to six. Both mono- and binuclear species were present in the asymmetric unit of **1** and **3**, while the asymmetric unit of **2** comprises two independent binuclear complexes. The antibacterial activities show that though the free ligand is inactive against *S. pyogenes* and *S. aureus*, complex **2** shows good activity against these bacteria; the antibacterial activity of **2** against *K. pneumonia* and *S. pyogenes* is higher than the standard antibiotic gentamicin.

Supplementary material

CCDC reference numbers 785010–785012 contain the supplementary crystallographic data for this article. These data can be obtained free of charge at www.ccdc.cam.ac.uk/conts/retrieving.html.

Acknowledgments

Support of this investigation by Payame Noor University is gratefully acknowledged by L.S. The MacDiarmid Institute is thanked for funding the purchase of the X-ray diffractometer.

References

[1] U.S. Schubert, C. Eschbaumer, P. Andres, H. Hofmeier, C.H. Weidl, E. Herdtweek, E. Dulkeith, A. Morteani, N.E. Hecker, J. Feldmann. *Synth. Met*., **121**, 1249 (2001).
[2] W. Huang, W. You, L. Wang, C. Yao. *Inorg. Chim. Acta*, **362**, 2127 (2009).

[3] W. You, W. Huang, Y. Fan, C. Yao. *J. Coord. Chem.*, **62**, 2125 (2009).
[4] (a) E.C. Constable, J. Lewis, M.C. Liptrot, P.R. Raithby. *Inorg. Chim. Acta*, **178**, 47 (1990); (b) E.C. Constable, S. Mundwilder. *Polyhedron*, **18**, 2433 (1999).
[5] H. Feng, X.P. Zhou, T. Wu, D. Li, Y.G. Yin, S.W. Ng. *Inorg. Chim. Acta*, **359**, 4027 (2006).
[6] R.A. Fallahpour. *Synthesis*, **155** (2003).
[7] (a) L. Gou, Q.R. Wu, H.M. Hu, T. Qin, G.L. Xue, M.L. Yang, Z.X. Tang. *Polyhedron*, **27**, 1517 (2008); (b) J.P. Lopez, W. Kraus, G. Reck, A. Thunemann, D.C. Kurth. *Inorg. Chem. Commun.*, **8**, 281 (2005).
[8] J.E. Beves, P. Chwalisz, E.C. Constable, C.E. Housecroft, M. Neuburger, S. Schaffner, J.A. Zampese. *Inorg. Chem. Commun.*, **11**, 1009 (2008).
[9] J. Wang, G.S. Hanan. *Synlett*, 1251 (2005).
[10] J.P. Colin, A. Jouaiti, J.P. Sauvage. *J. Electroanal. Chem.*, **286**, 75 (1990).
[11] J.M. Haider, M. Chavarot, S. Weinder, I. Sadler, R.M. Williams, L. De Cola, Z. Pikramenou. *Inorg. Chem.*, **40**, 3912 (2001).
[12] J. Chambers, B. Eaves, D. Parker, R. Claxton, P.S. Ray, S.J. Slattery. *Inorg. Chim. Acta*, **359**, 2400 (2006).
[13] S. Vaduvesca, P.G. Potvin. *Eur. J. Inorg. Chem.*, 1763 (2004).
[14] H.-G. Liu, Y.-C. Qiu, J.-Z. Wu. *Acta Crystallogr., Sect. E*, **63**, o4876 (2007).
[15] H.-G. Liu, Y.-C. Qiu, J.-Z. Wu. *Acta Crystallogr., Sect. E*, **63**, m2393 (2007).
[16] N. Yoshikawa, S. Yamabe, N. Kaneshia, Y. Kai, H. Takashima, K. Tsukahara. *Eur. J. Inorg. Chem.*, 1911 (2007).
[17] X.-P. Zhou, W.-X. Ni, S.-Z. Zhan, J. Ni, D. Li, Y.-G. Yin. *Inorg. Chem.*, **46**, 2345 (2007).
[18] L.A. Saghatforoush, F. Marandi, I. Pantenburg, G. Meyer. *Z. Anorg. Allg. Chem.*, **635**, 1523 (2009).
[19] F. Marandi, L.A. Saghatforoush, I. Pantenburg, G. Meyer. *J. Mol. Struct.*, **938**, 277 (2009).
[20] J. Granifo, M.T. Garland, R. Baggio. *Inorg. Chem. Commun.*, **7**, 77 (2004).
[21] W. Huang, G. Masuda, S. Maeda, H. Tanaka, H. Hino, T. Ogawa. *Inorg. Chem.*, **47** 468 (2008).
[22] W. Huang, H. Tanaka, T. Ogawa. *J. Phys. Chem.*, **C112**, 11513 (2008).
[23] G.M. Sheldrick. *SHELXL-97. Program for the Refinement of Crystal Structures*, University of Gottingen, Gottingen, Germany (1997).
[24] L.J. Farrugia. *J. Appl. Crystallogr.*, **30**, 565 (1997).
[25] Mercury 1.4.1, Copyright Cambridge Crystallographic Data Centre, 12 Union Road, Cambridge, CB2 1EZ, UK (2001).
[26] A. Baver, W.M.M. Kirby, J.E. Sherris, M. Turck. *Am. J. Clin. Pathol.*, **45**, 493 (1986).
[27] M.N. Indul, A.A.M. Hatha, C. Abirosh, U. Harsha, G. Vivekanandan. *Braz. J. Microbiol.*, **37**, 153 (2006).
[28] L. Shen, Y.Z. Xu. *J. Chem. Soc., Dalton Trans.*, 3413 (2001).
[29] K. Nakamoto. *Infrared and Raman Spectra of Inorganic and Coordination Compounds*, 4th Edn, Wiley, New York (1986).
[30] R. Cortes, J.L. Pizarro, L. Lezama, M.I. Arriortua, T. Rojo. *Inorg. Chem.*, **33**, 2697 (1994).
[31] D.H. Williams, I. Fleming. *Spectroscopic Methods in Organic Chemistry*, 4th Edn, McGraw Hill, London (1989).
[32] N. Li, L. Gou, H.M. Hu, S.H. Chen, X.L. Chen, B.C. Wang, Q.R. Wu, M.L. Yang, G.L. Xue. *Inorg. Chim. Acta*, **362**, 3475 (2009).
[33] N.W. Alcock, P.R. Barker, J.M. Haider, M.J. Hannon, C.L. Painting, Z. Pikramenou, E.A. Plummer, K. Rissanen, P. Saarenketo. *J. Chem. Soc., Dalton Trans.*, 1447 (2000).
[34] (a) G.R. Desiraju, T. Steiner. *The Weak Hydrogen Bond, IUCr Monograph on Crystallography*, Vol. 9, Oxford University Press, Oxford, UK (1999); (b) J. Granifo, M. Vargas, M.T. Garland, A. Ibanez, R. Gavino, R. Baggio. *Inorg. Chem. Commun.*, **11**, 1388 (2008).
[35] A.C. Moro, F.W. Watanabe, S.R. Ananias, A.E. Mauro, A.V.G. Netto, A.P.R. Lima, J.G. Ferreira, R.H.A. Santos. *Inorg. Chem. Commun.*, **9**, 493 (2006).
[36] J.W. Steed, J.L. Atwood. *Supramolecular Chemistry: A Concise Introduction*, John Wiley & Sons, Ltd., Chichester, UK (2000).
[37] C.A. Hollis, L.R. Hanton, J.C. Morris, C.J. Sumby. *Cryst. Growth Des.*, **9**, 2911 (2009).
[38] (a) T. Dorn, C. Janiak, K. Abu-Shandi. *Cryst. Eng. Comm.*, **7**, 633 (2005); (b) S. Banerjee, A. Ghosh, B. Wu, P.-G. Lassahn, C. Janiak. *Polyhedron*, **24**, 593 (2005); (c) R.D. Hancock, M.S. Shaikjee, S.M. Dobson, J.C.A. Boeyens. *Inorg. Chim. Acta*, **154**, 229 (1988); (d) I.G. Dance, M.L. Scudder. *J. Chem. Soc., Dalton Trans.*, 3755 (1996).
[39] Z. Shi, S.H. Feng, Y. Sun, J. Hua. *Inorg. Chem.*, **40**, 5312 (2001).
[40] K.J. Arm, W. Leslie, J.A.G. Williams. *Inorg. Chim. Acta*, **359**, 1222 (2006).
[41] W. Goodall, J.A.G. Williams. *J. Chem. Soc., Dalton Trans.*, 2893 (2000).
[42] E.C. Constable, C.E. Housecroft, M. Neuburger, S. Schaffner, F. Schaper. *Inorg. Chem. Commun.*, **9**, 433 (2006).
[43] C. Janiak. *J. Chem. Soc., Dalton Trans.*, 1527 (1999).

Downloaded by [Renmin University of China] at 10:21 13 October 2013

[44] J.C. Collings, K.P. Roscoe, E.G. Robins, A.S. Batsanov, L.M. Stimson, J.A.K. Howard, S.J. Clark, T.B. Marder. *New J. Chem.*, **26**, 1740 (2002).
[45] (a) L.A. Saghatforoush, F. Chalabian, A. Aminkhani, G. Karimnezhad, S. Ershad. *Eur. J. Med. Chem.*, **44**, 4490 (2009); (b) K.-B. Chew, M.T.H. Tarafder, K.A. Crouse, A.M. Ali, B.M. Yamin, H.-K. Fun. *Polyhedron*, **23**, 1385 (2004).
[46] S.D. Cummings. *Coord. Chem. Rev.*, **253**, 1495 (2009).
[47] A. Jain, B.S.J. Winkel, K.J. Brewer. *J. Inorg. Biochem.*, **101**, 1525 (2007).

Downloaded by [Renmin University of China] at 10:21 13 October 2013